


A developed flywheel energy storage with built-in rotating supercapacitors

Hamidreza TOODEJI* 

Department of Electrical Engineering, Yazd University, Yazd, Iran

Received: 26.03.2018

Accepted/Published Online: 17.09.2018

Final Version: 22.01.2019

Abstract: Flywheel energy storage can store large amounts of kinetic energy in its rotating parts, but its inertia restricts the rate of power exchange. On the other hand, there is supercapacitor with the ability of exchanging large amounts of instantaneous power. Therefore, the combination of these two systems can significantly improve the dynamic response of conventional flywheel energy storage. This paper proposes a novel design for this combined system in which supercapacitors are located inside the rotating disk. Therefore, supercapacitors can significantly improve the dynamic performance of the flywheel energy storage with trivial effects on its size and weight. Moreover, the ability of rotating supercapacitors to store electrical as well as kinetic energy increases the energy storage capacity of the proposed flywheel energy storage. This developed system with its improved performance can be widely employed instead of the conventional flywheel energy storage in various applications. In this paper, the proposed structures with built-in rotating supercapacitors are mechanically analyzed by CATIA and ABAQUS. In addition, the developed flywheel energy storage, which is equipped with a permanent magnet synchronous machine and its modified indirect vector controller, is simulated in MATLAB/Simulink under various conditions.

Key words: Flywheel energy storage, indirect vector control, permanent magnet synchronous machine, rotating supercapacitor, moment of inertia, stress and modal analysis

1. Introduction

Today, different energy storages, from very large to very small-scale systems, can be found in various applications [1–3]. In a power grid, utilizing energy storage results in numerous advantages like improving the power quality [4], smoothing the power fluctuations of renewable energy sources [5], and ensuring frequency stability of islanded microgrids [6]. On the other hand, there are vehicular applications that employ medium- and small-scale energy storage. Electric transportation, which attracts more attention due to the disadvantages of fossil fuels, utilizes energy storage to supply the driving force and also save regenerative braking energy [7–9]. As another vehicular application of energy storages, some spacecrafts are equipped with energy storage to save available solar energy and give it back in darkness [10–12].

Among different energy storage systems, electrochemical batteries are the most applicable ones due to their mature technology [13]. In some applications, a fuel cell system is employed that generates electricity from a chemical reaction between hydrogen and air. The produced water is then electrolyzed by electricity to extract hydrogen and charge the fuel cell again. However, an electrochemical battery may be utilized along with the fuel cell to improve its slow dynamic response. In an electric vehicle (EV), for example, the improved response of this combined energy storage helps to capture more braking energy and also assist in the acceleration of the vehicle

*Correspondence: toodeji@yazd.ac.ir

when the fuel cell stack is warming up [14, 15]. Flywheel energy storage is another storage system that converts electrical energy into mechanical energy via an electrical machine and stores the kinetic energy in a rotating disk. In the discharge mode, this stored energy is given back by generator operation of the electrical machine. This highly efficient energy storage can exchange considerable amounts of energy over a short time interval in comparison with electrochemical batteries. Moreover, its high-cycle characteristic, which is independent of the temperature or depth of charge, makes this energy storage an attractive choice for various applications [16].

On the other hand, there are energy storages that can exchange considerable amounts of instantaneous power, but their energy storage capacity is relatively small. An obvious example is the supercapacitor with its attractive characteristics such as high capacity up to 5000 F and high cycle [17]. Due to the high power density of this supplementary device, the supercapacitor is usually employed beside other slow-response energy storages to improve their dynamic performance. Therefore, the stationary combination of a supercapacitor with an electrochemical battery or flywheel energy storage can be found in previous studies. Vehicular applications are examples of utilizing such combined energy storage systems. In such applications, small and light energy storages with high energy as well as high power density per mass and volume units are more preferred [18].

In this paper, a novel rotary combination of a supercapacitor and flywheel energy storage is proposed. By inserting supercapacitors inside the rotating disk, the developed flywheel energy storage with attractive characteristics is obtained. Moreover, merging supercapacitors into the rotating disk significantly reduces the size and weight of the proposed system compared with their stationary combination. This makes the proposed system suitable for vehicular applications in which the size as well as weight of the utilized energy storage is a real problem. Moreover, the proposed system with its improved dynamic response and higher energy storage capacity can be employed instead of conventional flywheel energy storage.

This paper is organized as follows; the flywheel and supercapacitor energy storages are respectively explained in the next two sections. The configuration of the proposed flywheel energy storage is presented and explained in Section 4. In this section, two mechanical structures are proposed for rotary combination of the disk and supercapacitors, and then the conventional indirect vector control of the permanent magnet synchronous machine (PMSM) is modified to coordinate the operation of the flywheel and supercapacitors for storing/supplying energy. Finally, the proposed disk structures are mechanically analyzed by CATIA and ABAQUS and then the proposed flywheel energy storage is simulated from an electrical viewpoint in MATLAB/Simulink under various conditions.

2. Flywheel energy storage

Flywheel energy storage is a mechanical battery that stores the kinetic energy in a rotating mass. Such a system consists of an electrical machine and its driver for energy conversion and a rotating mass for storing kinetic energy [16, 19]. The electrical machine in the charging mode operates as a motor and converts electrical into mechanical energy. Storing this converted energy in the rotating disk consequently increases its speed. During the discharge mode, the generator operation of the electrical machine returns the stored kinetic energy and the speed is reduced accordingly. Therefore, Eq. (1) shows that the rotational speed (ω) can be chosen as a straightforward index for measuring the stored energy or the state of charge (SOC) of a rotating mass [20].

$$E_{flywheel} = \frac{1}{2} J \omega^2 \quad (1)$$

Here, J and ω are the moment of inertia and angular velocity of the disk, respectively. This equation also shows that a high-speed disk with higher moment of inertia can store larger amounts of energy. Higher moments of inertia can be obtained by selection of appropriate shapes and materials for the disk. Moreover, higher speeds can be achieved by a light material with low density and high tensile strength characteristics, e.g., advanced composite materials. Such characteristics increase the maximum stored energy per volume unit (J/m^3) as well mass unit (J/kg) significantly.

Based on the maximum speed of the rotating disk, flywheel energy storage systems can be divided into low- and high-speed groups. In low-speed metallic disks with high density as well as low tensile strength, significant energy storage density cannot be obtained due to the limitation of speed increasing. However, the cost of a metallic disk is meaningfully lower than advanced composite ones [19].

From the electrical machine viewpoint, different types such as induction machines, PMSM, and switched reluctance machines have been employed in flywheel energy storages. Due to the simple structure, lower cost, and higher torque of induction machines, they have usually been employed in low-speed and high-power flywheel energy storages. The PMSM, as a highly efficient and controllable machine with negligible rotor losses, is a good choice for high-speed and medium-power applications [21, 22]. It is worth mentioning that in the newer generation of flywheels, which are known as integrated designs, the electromagnetic rotor and energy storage part are combined. However, this design is not suitable for composite rotors due to the need for an electromagnetic material for an electrical machine [19, 23]. Besides these various electrical machines, different electrical drivers have also been introduced to control the motor/generator operation as well as the speed of the utilized electrical machine.

The windage losses of rotating parts as well as bearings' frictional losses result in a high self-discharging rate, up to 20% of stored energy, in different flywheel energy storage systems [19]. Therefore, this energy storage system cannot be solely employed for long-term energy storage in comparison with other systems such as electrochemical batteries. However, magnetic bearings as well as vacuum housing are employed in high-speed applications to reduce aerodynamic drag, windage, and friction significantly [23, 24].

3. Supercapacitor energy storage

Eq. (2) shows that the stored energy of a capacitor is in proportion with its squared voltage as well as its capacity. On the other hand, high surface area electrodes in the supercapacitor, which is also called an ultracapacitor or double-layer capacitor, increase the capacity. As a result, the supercapacitor can be utilized as a promising energy storage device.

$$E_{\text{capacitor}} = \frac{1}{2} C V^2 \quad (2)$$

Here, C and V are the capacity and voltage of the capacitor, respectively. Porous active carbon is usually employed in high area surface electrodes, whereas aerogel carbon or carbon nanotubes can also be utilized. However, ultrahigh capacities up to 5000 F in commercial supercapacitors have been reached by active carbon. In addition, utilization of some other materials such as metal oxide or conductive polymers have also been considered [25]. From the electrolyte viewpoint, supercapacitors can be categorized into organic and aqueous groups; higher nominal voltage of about 3 V can be reached in the former, whereas the breakdown voltage of the latter is limited to about 1 V. These low nominal voltages make using series-parallel connections of supercapacitors necessary to obtain a desired nominal voltage [26].

In contrast with the electrochemical battery that stores energy through a reversible chemical reaction,

the supercapacitor experiences no chemical reaction. In consequence, charging cycles of the supercapacitor are almost unlimited and the deep cycle has almost no impact on its lifetime. However, due to the direct relation of the supercapacitor's SOC with its terminal voltage, the deep cycle means wide variation of the terminal voltage. To counter this variation, the operating point of the supercapacitor should be limited to the high SOC region or, alternatively, an intermediate converter should be employed to fix the output voltage.

Since the area of the conductive path specifies current density, high current can be achieved in the supercapacitor due to its large surface area electrodes. Therefore, high power density per mass as well as volume units of about 2–5 kW/kg and 20–30 kW/m³ can be reached, respectively. Such fast dynamic response introduces the supercapacitor as auxiliary energy storage for absorbing/supplying pulsed power. For example, most of the braking energy of an EV can be absorbed and sudden power demand during vehicle acceleration can be supplied by employing supercapacitors.

In contrast, the energy storage densities of supercapacitors per mass and volume units are about 2–5 Wh/kg and 10,000 Wh/m³, respectively. These low amounts are due to difficult access of ions to the porous surface of electrodes. Moreover, a notable self-discharge rate of the supercapacitor, about 14%, makes it inappropriate for long-term energy storage in comparison with the electrochemical battery. In addition, the high cost of the supercapacitor, which can reach up to 9500 \$/kWh, is a disadvantage that would expectedly be reduced in the future [26].

4. The proposed flywheel energy storage

As was mentioned, the flywheel energy storage can store considerable amounts of energy, but its power exchange rate is restricted. On the other hand, there is the supercapacitor with fast dynamic response. Therefore, the immediate consequence of the combination of these two systems is a developed flywheel energy storage with improved dynamic response. However, employing stationary supercapacitors besides the conventional flywheel energy storage has been considered before, but in the proposed system, supercapacitors are put inside the rotating disk. Accordingly, these rotating supercapacitors have negligible impact on the size as well as the weight of any conventional flywheel energy storage.

The electrical configuration of the proposed flywheel energy storage is presented in Figure 1. In this configuration, a common DC bus is utilized as an intermediate for power exchange between connected elements. As is seen, the PMSM and rotating series-parallel supercapacitors are connected to the DC bus through a VSC and a contactless power transfer system, respectively. The presented energy source, which supplies the common DC bus, is a photovoltaic (PV) system that is controlled by a DC-DC converter aiming to extract maximum available solar power. It is obvious that other energy sources can also be employed instead of the PV energy conversion system. Since the voltage of the common DC bus may be slightly varied, the voltage of sensitive DC loads is regulated by a DC-DC converter while other DC loads are directly connected to the common DC bus. These connected elements establish a standalone system that can be utilized in mobile applications such as electric vehicles, spacecrafts, ships, etc. The proposed flywheel energy storage can also be employed in on-grid applications, regardless of the existence of DC sources/loads. For this purpose, the common DC bus is connected to the AC grid/AC loads via a DC-AC converter, as is shown by the dotted line at the bottom left of Figure 1.

In the proposed combined system, rotating supercapacitors cannot be directly connected to the common DC bus. Employing slip rings and brushes to imitate a wound rotor induction machine leads to intolerable frictional losses in the high speeds. Moreover, transferring the produced heat in the vacuum housing is more

difficult. Therefore, a contactless power transfer system is utilized to overcome these serious problems. As is presented in the bottom of Figure 1, this system consists of a coupling rotary transformer, which was introduced in [27], as well as a bidirectional resonant converter that was proposed in [28]. The rotary transformer is a detached magnetic coupling structure with an axial symmetry and an air-gap between the primary and secondary side [27]. In addition, the high frequency resonant converter is employed to reduce the size of the rotary transformer. It should be noted that the resonant converter has zero-voltage switching (ZVS) ability, so its switching losses are significantly reduced [28]. Besides, a wireless communication link between rotary and stationary converters is utilized in this contactless system.

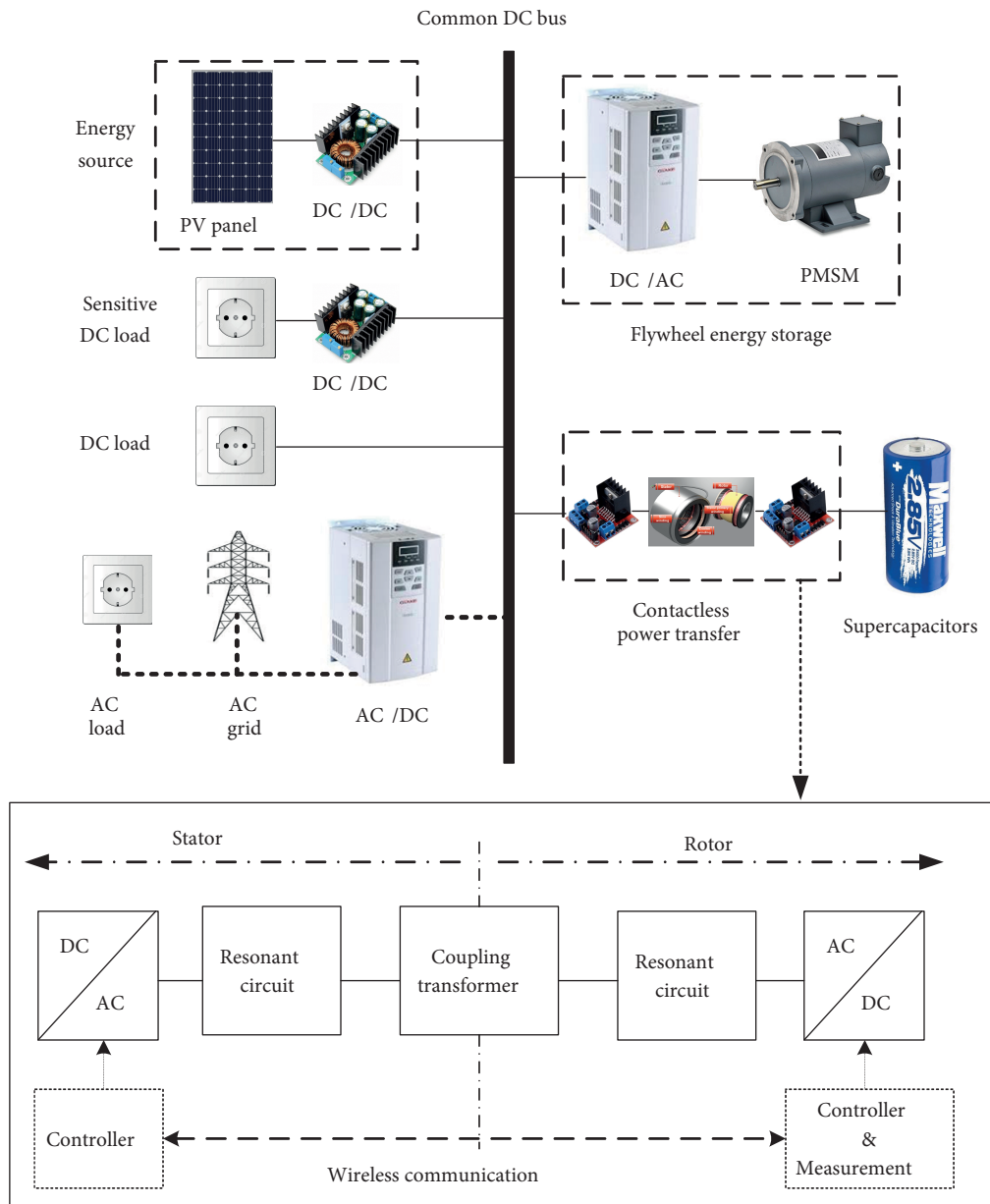


Figure 1. The electrical configuration of the proposed flywheel energy storage.

It is worth mentioning that, from the mechanical viewpoint, magnetic bearings and vacuum housing are employed in the proposed energy storage, similar to other high-speed flywheel energy storages [23]. In the following two subsections, the mechanical design of the proposed structure and the modified vector control of the PMSM are considered, respectively.

4.1. Disk design

In the proposed flywheel energy storage, supercapacitors are placed in the predicted holes of the rotating disk, so the disk size remains almost unchanged. Moreover, the weight of the proposed system also shows trivial change due to the similarity of utilized materials in the supercapacitor and rotating composite disk. In addition, rotating supercapacitors can store electrical energy as well as kinetic energy. The developed flywheel energy storage, therefore, exhibits higher energy storage capacity as well as faster dynamic response, with a trivial change in the size and weight, compared with conventional flywheel systems.

Among different possible ways to insert supercapacitors inside the disk, those designs that maximize kinetic energy storage capacity are preferred. Considering Eq. (1) shows that a high-speed disk with higher moment of inertia is more desired. To obtain higher moment of inertia, mass distance to the rotation axis should be as great as possible (see Eq. (3)) [20].

$$J = \int r^2 \cdot dm \quad (3)$$

Here, r is the distance of the differential element of mass (dm) to the rotation axis. Accordingly, supercapacitors should be placed as far as possible from the rotation axis to obtain higher moment of inertia. Therefore, the circumference of the disk is the best choice for inserting supercapacitors, as presented in Figure 2a. However, this choice for a large number of supercapacitors results in a very large-radius disk. Thus, other alternative designs such as concentric circles, multiple stages, or their combinations can be employed considering the number of supercapacitors as well as space limitations of the rotating disk.

A concentric-circles design with ten supercapacitors is presented in Figure 2b. It is clear that this structure, compared with the other, leads to smaller moment of inertia and consequently lower kinetic energy storage capacity. Indeed, this is a trade-off between the disk size and its storage capacity in the case of limited space for the rotating disk.

Another important factor is maximum allowable tension of the disk, which specifies the maximum rotating speed and consequently the kinetic energy storage capacity. The energy density of the rotating disk per volume and mass units is defined by Eq. (4) [29].

$$e_v = K \cdot \sigma_a \quad , \quad e_m = K \cdot \frac{\sigma_a}{\rho} \quad (4)$$

Here, e_v and e_m are energy density per volume and mass units, K is shape factor, density is shown by ρ , and σ_a represents maximum allowable tension. These equations show that higher energy storage density can be reached by lightweight and high-tensile strength materials. Metals, as dense materials with low tensile strength, are in contrast with advanced low density composite materials with high tensile strength such as graphite HS/epoxy [30]. Based on these characteristics, metals are appropriate for low-speed disks while the composite materials are suitable for high-speed applications.

Since the shape factor depends on the disk geometry, this amount tends to be 0.5 for a thin ring structure, which is constructed from composite materials. Thus, the inner hole in the proposed main structure is predicted

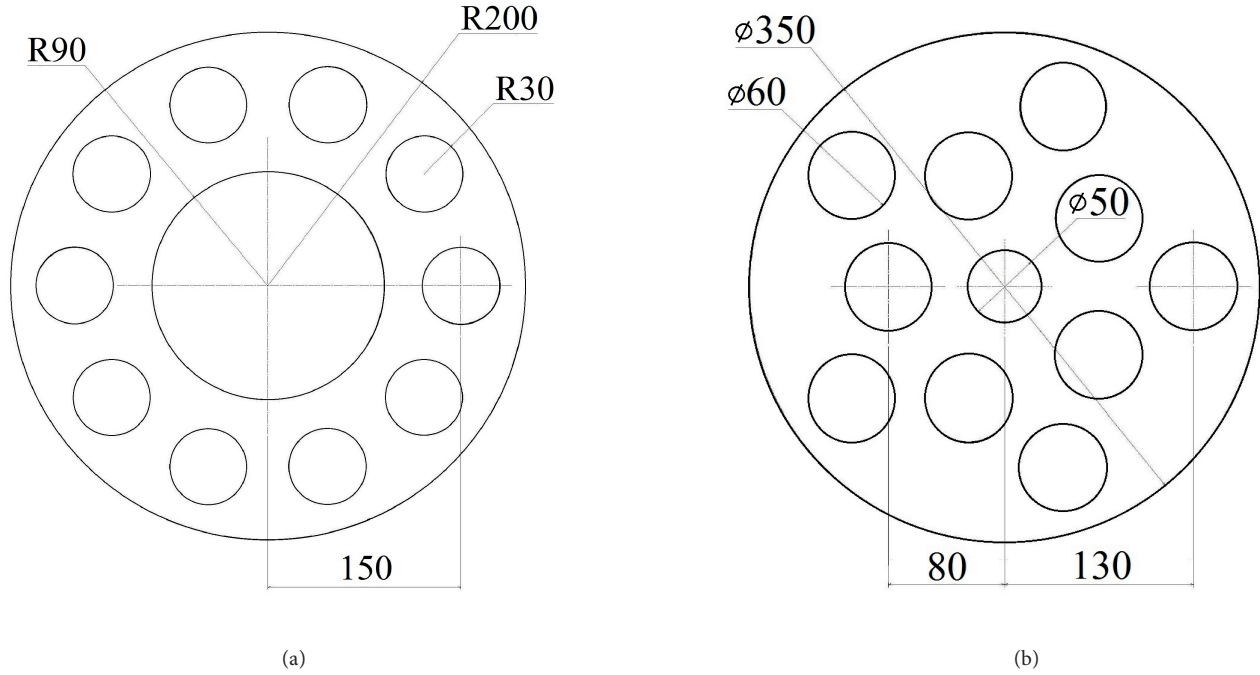


Figure 2. A disk with ten holes: (a) main, (b) concentric-circles structures.

to increase the shape factor. It seems that this inner empty space reduces the moment of inertia if only Eqs. (2) and (3) are considered. However, more attention to Eq. (4) reveals that a solid composite disk with lower shape factor results in lower energy storage density per volume and mass units. This can justify the lower energy density of the concentric-circles structure as a result of its lower shape factor.

4.2. Modified indirect vector control of PMSM

Figure 3 presents the block diagram of the modified indirect vector control of the PMSM, which is employed in the proposed flywheel energy storage. The brief description of conventional vector control, which is also known as field oriented control, is as follows [31]. By assumption of sinusoidal excitation, voltage equations of a PMSM in the stationary reference frame are:

$$v_a = R_s i_a + \frac{d\lambda_a}{dt}, \quad v_b = R_s i_b + \frac{d\lambda_b}{dt}, \quad v_c = R_s i_c + \frac{d\lambda_c}{dt} \quad (5)$$

Here, R_s is stator winding resistance; λ_a , λ_b , and λ_c are the flux linkages; and v_a , v_b , and v_c are the voltage of phases a , b , and c , respectively. By applying Park–Clarke orthogonal transformation in which the rotating frame is attached to the rotor, the voltage equations are transformed to $dq\theta$ coordinates.

$$v_d = R_s i_d + \frac{d}{dt} \lambda_d - \lambda_q \frac{d\theta}{dt}, \quad v_q = R_s i_q + \frac{d}{dt} \lambda_q + \lambda_d \frac{d\theta}{dt}, \quad v_0 = R_s i_0 + \frac{d}{dt} \lambda_0 \quad (6)$$

Here, θ is the angle between stationary and rotating reference frames. v_d , v_q , and v_0 are the phase voltages; phase currents are represented by i_d , i_q , and i_0 ; and λ_d , λ_q , and λ_0 are the phase flux linkages, all in $dq\theta$ coordinates. The flux linkages of the d - and q -axes are equal to:

$$\lambda_d = L_d i_d + \lambda_m, \quad \lambda_q = L_q i_q \quad (7)$$

Here, L_d and L_q are the constant d - and q -axes inductances, respectively, and λ_m is the flux linkage that is produced by the permanent magnets of the rotor. By assumption of well-balanced three-phase windings, the voltage equation of the zero-axis can be ignored. Therefore, substitution of Eq. (7) in Eq. (6) results in:

$$v_d = R_s i_d + L_d \frac{di_d}{dt} - L_q i_q \frac{d\theta}{dt}, \quad v_q = R_s i_q + L_q \frac{di_q}{dt} + (L_d i_d + \lambda_m) \frac{d\theta}{dt} \quad (8)$$

After applying transformation, the torque equation is obtained:

$$T_e = \frac{3}{2} p (\lambda_d i_q - \lambda_q i_d) = \frac{3}{2} p (\lambda_m i_q + (L_d - L_q) i_d i_q) \quad (9)$$

Here, p is the number of pole pairs. Since the flux and torque control are decoupled, the q -axis current is controlled to produce sufficient torque while the air-gap flux linkage is modified by the d -axis current. In normal operation, the d -axis current is set to zero to achieve the maximum torque-to-ampere ratio. Therefore, the reference speed value is the main input of the conventional field oriented control while the electromagnetic torque and rotor speed are its outputs. As presented in Figure 3, current and speed feedback loops are added to provide the desired performance. Thus, output of the speed PI controller is the reference value for the q -axis current.

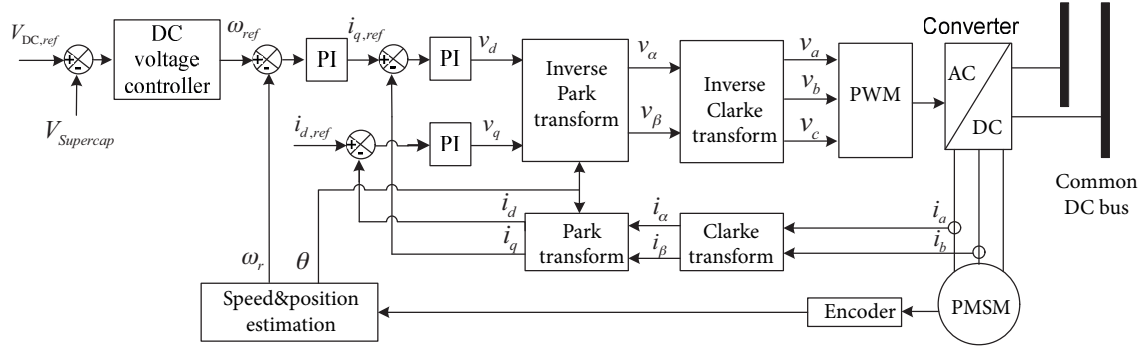


Figure 3. Block diagram of the modified indirect vector control of the PMSM.

The mentioned conventional indirect vector control, which governs the rotating speed of the PMSM, should be modified to coordinate the operation of the flywheel and supercapacitors for storing/supplying energy. For this purpose, the priority of energy exchange is given to the supercapacitors, as the electrical energy storage part, and the kinetic energy storage part is employed in the next stage when it is required. The flowchart of the proposed DC voltage controller, as the modification of conventional indirect vector control, is presented in Figure 4.

For small energy exchanges, the difference between the reference ($V_{DC,ref}$) and resultant voltage of supercapacitors ($V_{Supercap}$) will be smaller than the threshold voltage (V_{th}). Consequently, the PI controller does not operate and the reference speed value (ω_{ref}) does not change. For large amounts of energy exchanges, the resultant voltage of supercapacitors crosses the threshold voltage and activates the PI controller. As a result, $V_{Supercap}$ is conducted to the reference value, but with a small steady-state error (ϵ) preventing unfavorable operations of the controller. Then the PI controller is deactivated and the last generated reference speed is continually given to the speed controller.

By the proposed DC voltage controller, received energy in the charging mode is stored with fast dynamics in the rotating supercapacitors electrically. Receiving more energy leads to trespassing on the upper threshold

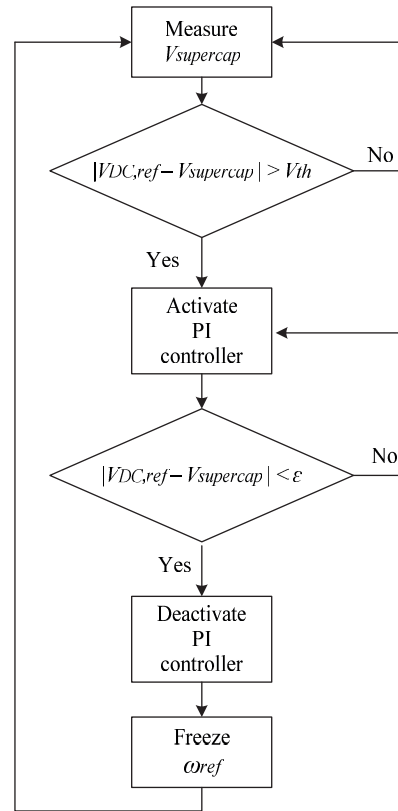


Figure 4. Flowchart of proposed DC voltage controller.

voltage, which activates the PI controller, and consequently the disk speed increases to store this extra energy in the form of kinetic energy. In the discharging mode, the demanded energy is directly supplied by the stored electrical energy of supercapacitors without any change in the disk speed. Demanding more energy decreases the DC voltage below the lower threshold voltage and activates the PI controller. In consequence, the speed is reduced to give back the stored kinetic energy.

It should be noted that broad allowable voltage variations by choosing large threshold values restrict the kinetic energy exchange to a large amount of power. Accordingly, fast dynamic response to small power exchanges with no need to change speed is obtained. However, the side effects of these larger DC voltage variations on other equipment should also be considered. As a solution for these large variations, a DC-DC converter can be employed for sensitive DC loads, as is presented in the proposed flywheel energy storage. Finally, it is worth mentioning that energy exchange with rotating parts needs energy conversion by a nonideal PMSM. Therefore, employing only supercapacitors for small power exchanges increases the total efficiency of the proposed system.

4.3. Discussion

The proposed idea for inserting the supercapacitor inside the rotating disk would face some limitations in low-speed and ultrahigh-speed flywheel energy storages. For low-speed systems in which metallic disks have been commonly utilized, putting supercapacitors may decrease the total energy storage capacity. This is the result of filling the holes of the metallic disk with a lower density material. However, the electrical energy storage capacity

of supercapacitors may alleviate this energy storage deficiency. In addition, the lower density of supercapacitors decreases the total weight of the rotating disk. Moreover, the fast response ability of this low-speed system to exchange pulsed power should be considered.

In contrast, there are ultrahigh-speed flywheel energy storages. Due to the similarity of the disk and the supercapacitor's material, inserting supercapacitors inside the rotating part does not significantly affect the kinetic energy storage capacity. However, the electromagnetic interference due to the rotation of charged supercapacitors should be precisely studied.

5. Simulation results

In this part, the proposed disk structures are simulated in CATIA and ABAQUS for mechanical design analysis. Afterwards, the proposed flywheel energy storage is electrically simulated in MATLAB/Simulink under various conditions to verify its claimed abilities.

5.1. Mechanical design analysis of the proposed disk structures

To compare the proposed structures with a conventional solid disk, their moments of inertia are first calculated. The solid disk is similar to the main structure, but with no hole. For the sake of comparison, similar material is utilized for the solid disk and both proposed structures. Calculating the moment of inertia for the solid disk is straightforward, but for the proposed structures, the moment of inertia should be obtained by the parallel axes theorem:

$$J = J_0 + mr^2 \quad (10)$$

Here, J_0 is the moment of inertia of mass m around its symmetry axis and r is the distance between symmetry and its parallel rotation axis. To use this theorem, one isolated supercapacitor and the holed disk are separately considered and then the total moment of inertia is calculated. Indeed, each supercapacitor in the proposed structures rotates around the disk axis, which is in parallel with its symmetry axis.

Both proposed disk structures are assembled in CATIA while composite graphite HS/epoxy material with density 2000 kg/m^3 and maximum tensile strength 1000 MPa is selected. The commercial supercapacitor DuraBlue of Maxwell Technologies Inc. with capacity 3400 F and density 1420 kg/m^3 is considered here [32]. Table 1 presents the obtained mechanical parameters of different structures, which are calculated by CATIA. Since there are two circles in the concentric-circles structure, two radii are given for this structure in Table 1.

The next step is finding the maximum speed of each proposed structure, which depends on the maximum tensile strength as well as disk shape. For this purpose, ABAQUS is employed for stress analysis of these structures, which are rotated at 3000 rad/s . The obtained results for main and concentric circle structures are presented in Figures 5a and 5b, respectively.

Stress analysis of the concentric-circle structure shows unacceptable deformation of empty holes due to exerted tension. Besides, considering the supercapacitors in holes increases the tension and consequently severe deformation would be expected. Such high tension, about 815 MPa , can break the disk down and the hole deformation also can destroy the supercapacitors, so the maximum allowable speed of this structure is reduced to 2000 rad/s . In contrast, maximum calculated tension of the main structure, even with considering supercapacitors in the holes, is about 454 MPa , which is far from the tensile strength of the selected material (1000 MPa). This structure, therefore, can rotate at higher speeds, despite considering 3000 rad/s as its speed limit. Such a conservative margin of safety can cover the extra force on the holes' walls, which is exerted by supercapacitors, and dynamic tensions that appear as a result of speed changing.

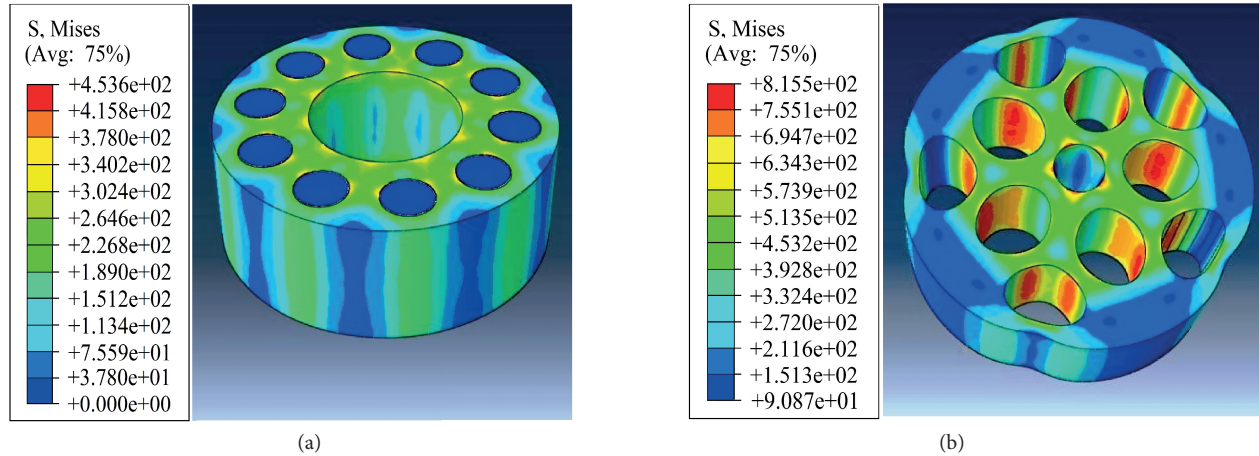


Figure 5. The results of stress analysis for (a) main and (b) concentric-circle structures.

Table 1. Calculated mechanical parameters of proposed and conventional structures.

	Moment of inertia without supercapacitors	Moment of inertia for one supercapacitor	Distance between rotation and symmetry axes	Total moment of inertia	Total mass	Total volume
Conventional solid structure	0.66522 kg.m ²	-	-	0.66522 kgm ²	27.66 kg	0.01383 m ³
Main structure	0.458 kg.m ²	2.349e-4 kg.m ²	150 mm	0.73295 kgm ²	23.925 kg	0.01267 m ³
Concentric circles structure	0.294 kg.m ²	2.349e-4 kgm ²	80, 130 mm	0.436626 kg.m ²	22.373 kg	0.01267 m ³

The resonant frequency of the proposed disk structures is an important issue that needs more attention, especially for high-speed applications. Operating near resonant frequency can lead to large vibration amplitudes, so the electromagnetic frequency of the rotating disk should be designed well below this resonant frequency. Modal analysis, which is commonly performed by finite element method (FEM), is utilized to calculate the resonance frequency. However, it is only necessary to carry out the first-order modal analysis and compare the obtained frequency with the electromagnetic one [33]. The first-order resonant frequencies of the main and concentric-cycle structures in vacuum, which are calculated by ABAQUS, are about 1342.4 Hz and 1128.6 Hz, respectively. It can be seen that these resonant frequency are acceptably higher than the nominal speed of the PMSM in Table 4 (3500 rad/s = 557.04 cycles/s = 557.04 Hz), as the highest speed of rotating disk.

Table 2 shows the energy storage density of each structure per mass and volume units, which are calculated by considering the maximum allowable speed as well as the results of Table 1. To compare with the conventional solid disk, its maximum speed is also assumed as 3000 rad/s, similar to that of the main proposed structure.

Table 2 reveals that the kinetic energy storage densities of the main structure per both mass and volume units are higher than the conventional structure. Moreover, lower kinetic energy density of the concentric-circles structure is a result of its lower moment of inertia as well as its smaller allowable speed. It should be noted that Table 2 shows only the kinetic energy storage density of the proposed structures, without considering the electrical energy storage capacity of the supercapacitors. Taking this extra energy storage capacity into account by Eq. (2) results in Table 3, which presents the total energy storage density of the conventional and proposed

Table 2. The kinetic energy density per mass and volume units for conventional and proposed structures.

	Maximum stored kinetic energy	Kinetic energy density per mass unit	Kinetic energy density per volume unit
Conventional solid structure	2,993,503 J	108.2 kJ/kg	216.5 MJ/kg
Main structure	3,298,275 J	138 kJ/kg	260.3 MJ/m ³
Concentric-circles structure	873,252 J	39 kJ/kg	68.9 MJ/m ³

structures. This table reveals that the stored energy capacity of the main structure is significantly higher than that of the conventional solid disk.

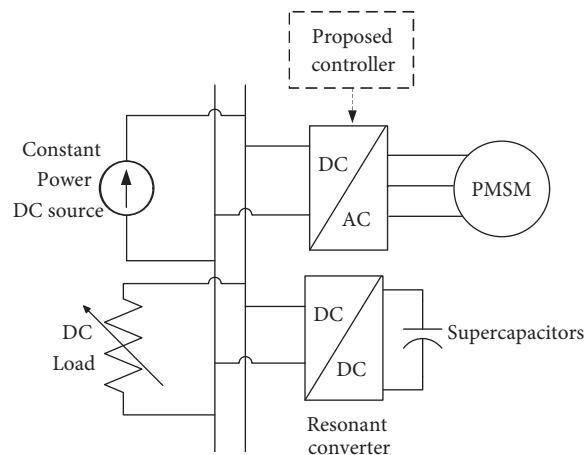
Table 3. Total energy storage density per mass and volume units for proposed structures.

	Total energy storage capacity	Total energy density per mass unit	Total energy density per volume unit
Main structure	3,440,419 J	143.8 kJ/kg	271.5 MJ/m ³
Concentric-circles structure	1,015,396 J	45.4 kJ/kg	80.1 MJ/m ³

It should be mentioned that the margin of safety for the main proposed structure is conservatively selected, so higher energy storage density can be reached by considering a narrower margin. Moreover, the assumption of similar speed for both the conventional and main proposed structures only helps to compare these structures, while the conventional structure can rotate at higher speeds and store more kinetic energy.

5.2. Electrical analysis of the proposed flywheel energy storage

In this section, the proposed flywheel energy storage with given electrical parameters in Table 4 is simulated in MATLAB/Simulink under various conditions. The utilized simulation model is shown in Figure 6, in which converters are considered lossless.

**Figure 6.** The utilized simulation model of the proposed flywheel energy storage.

This test system employs the proposed main structure with previously calculated parameters as its rotating disk. DC source and loads are connected to the common DC bus and exchange their energy with this bus. Due to incompatibility of the resultant voltage of supercapacitors with that of the common DC bus, the bidirectional resonant converter is considered as a DC-DC converter in the simulation model. To generalize the results, typical source and load with varying nature are considered. The generated power of solar PV panels in a spacecraft and the braking energy of an EV are examples of an energy source with varying nature.

Table 4. The electrical parameters of the test system.

PMSM	Nominal power	5 kW
	Nominal voltage	250 V
	Nominal speed	3500 rad/s
Supercapacitors	Number of serried supercapacitors	10
	Capacity of each supercapacitor	3400 F
	Nominal voltage of each supercapacitor	2.85 V
DC voltage controller	V_{th}	0.2 V
	ϵ	0.01 V
Common DC bus	Nominal voltage	280 V

Figure 7a shows the algebraic sum of the source and load's powers, so negative net power means more power generation in comparison with power consumption and vice versa. It is clear that the zero net power in this figure means the equality of generated and consumed power. At $t = 0.5$ s a sudden power generation with constant value occurs and lasts for 0.5 s. Recovered braking energy of an EV or generated power of PV panels in a spacecraft, which are suddenly exposed to sunlight, are examples of such condition. Figures 7b and 8a show that absorption of this available power by supercapacitors increases their resultant voltage. Moreover, it is seen that the common DC bus and supercapacitors in Figures 8a and 8b experience similar voltage variations. As a result of this incremental voltage, the upper threshold voltage is passed at $t = 0.7$ s. In consequence, the modified electrical driver tries to store this continued extra energy in the rotating disk and also returns the resultant voltage back to the nominal value, but with a predefined steady-state error (ϵ). Accordingly, the PMSM starts to accelerate for absorbing this continued extra power as well as a portion of stored electrical energy of supercapacitors. The active power variations of the PMSM decreasing the resultant DC voltage and increasing the disk speed in simulation results demonstrate this condition precisely. Before reaching the upper threshold voltage, the PMSM expectedly has no power exchange and available energy is completely absorbed by the supercapacitors. Therefore, the proposed flywheel energy storage can store almost all the available energy, e.g., the braking energy of an EV, with fast dynamic response.

With a stepped demand at $t = 2$ s the supercapacitors solely supply the load by stored electrical energy and consequently their resultant voltage decreases. Moreover, it is seen that before $t = 0.23$ s, when DC voltage reduces below the lower threshold voltage, the PMSM does not experience any power exchange. However, after passing this threshold, the speed is reduced to supply the load and also regulate the resultant voltage at the nominal value, but with a steady-state error (ϵ). This can explain the increasing resultant voltage of supercapacitors as well as decreasing speed of the PMSM, respectively. As seen in Figure 9a, the speed decrease continues even after finishing the stepped demand at $t = 3$ s. In fact, the stored kinetic energy is being converted to electrical energy and delivered to supercapacitors, returning the resultant voltage to the nominal value.

In spite of the fact that the voltage variations of the common DC bus are limited to 0.7%, the DC-DC converter can be employed to regulate the supply voltage of sensitive loads, as presented in the proposed flywheel

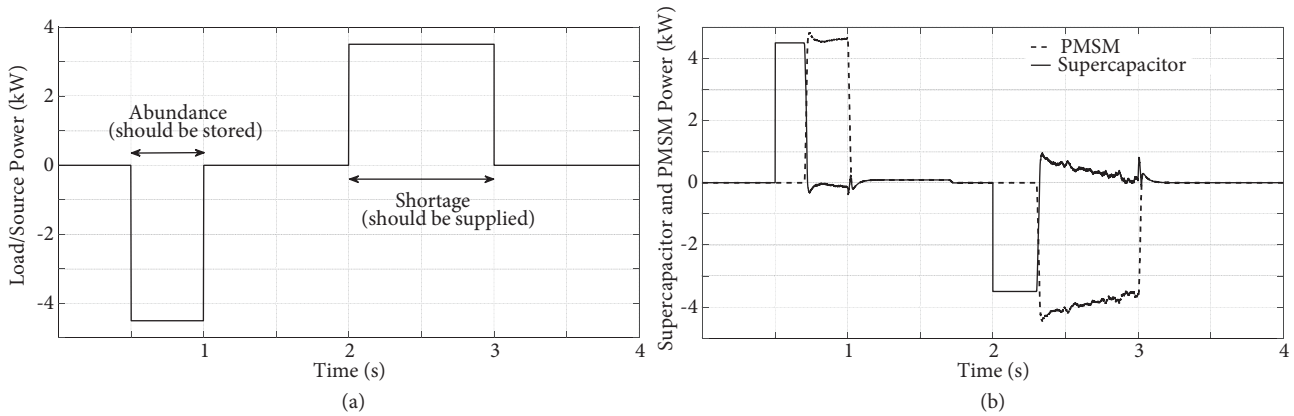


Figure 7. (a) Net generated/consumed power profile in the test system, (b) absorbed/generated power of PMSM and supercapacitors.

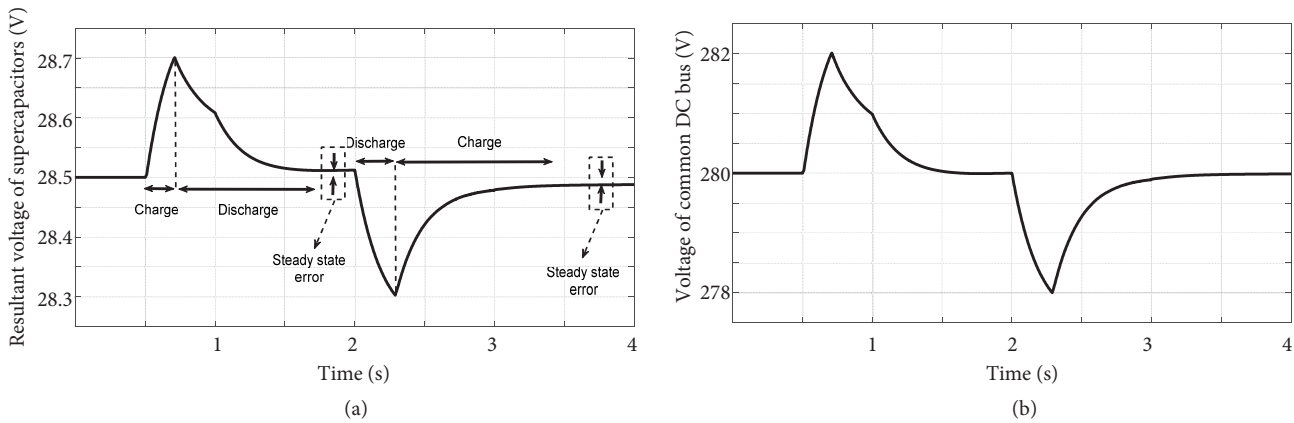


Figure 8. The voltage of (a) supercapacitors, (b) common DC bus.

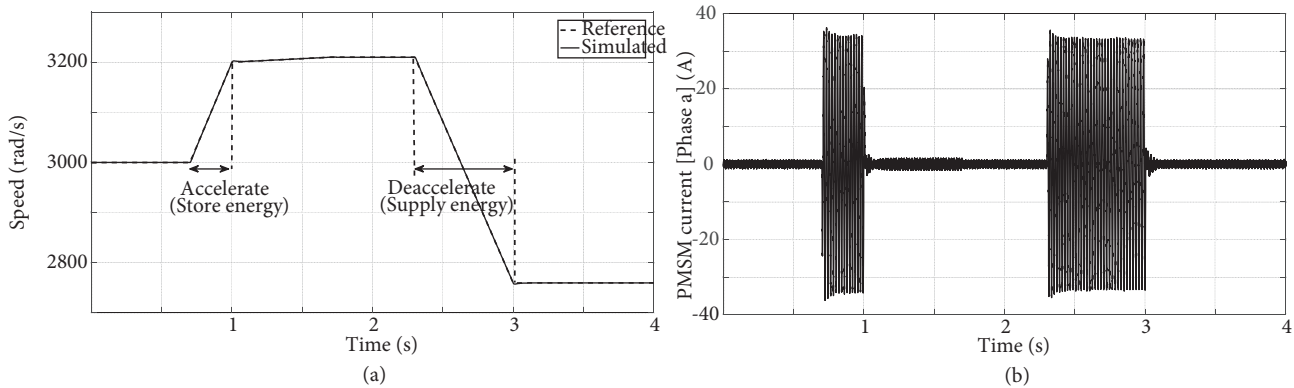


Figure 9. (a) Speed variations of PMSM and (b) stator current (phase a).

energy storage. It is worth mentioning that there is no steady-state error (ϵ) in the voltage of the supercapacitors compared with the common DC bus, due to the ability of the bidirectional resonant converter for independent voltage regulation of its two ends. As a result, the voltage of the common DC bus is simply regulated at its nominal value while the supercapacitors experience steady-state error. Figure 9b, which presents the one-phase

current of the PMSM, is consistent with its absorbed/generated power as well as its speed variations. As is expected, large amounts of current during acceleration and deceleration of the PMSM for absorbing and supplying energy, respectively, can be seen in Figure 9b.

These simulation results obviously show the fast dynamic response of the proposed flywheel energy storage from an electrical viewpoint. In comparison with the conventional flywheel energy storage, using such a fast dynamic system can supply/absorb pulsed power. This characteristic in electric transportation, for example, leads to higher acceleration and also receiving more braking energy that significantly increases the efficiency.

6. Conclusion

Energy storage density of the flywheel energy storage is very high, but the inertia of its rotating disk prevents exchanging large amounts of instantaneous power. On the other hand, the supercapacitor can easily exchange pulsed power. Therefore, the ability of exchanging pulsed power as well as storing high amounts of energy can be achieved by the combination of the supercapacitor with the conventional flywheel energy storage. In the proposed flywheel energy storage the supercapacitors are inserted into the rotating disk to improve the dynamic response. Interestingly, this scheme has trivial impact on the size and weight of the proposed system in comparison with similar conventional flywheel energy storage. Moreover, the electrical energy storage ability of rotating supercapacitors, besides the storage of kinetic energy, increases the total energy storage density significantly. In the proposed flywheel energy storage, a modified indirect vector control is employed for the utilized PMSM to give the priority of energy exchange to supercapacitors. In this introduced strategy, a small amount of power is directly supplied/absorbed by supercapacitors with fast dynamic response and exchanging the kinetic energy is dedicated to large power variations. Preventing the proposed flywheel energy storage from unnecessary speed changes for small amounts of power increases the performance and its efficiency. In this paper, the mechanical characteristics of the proposed and conventional disk structures are calculated by CATIA and mechanical design analysis of these structures is performed by FEM in ABAQUS. In addition, a test system is simulated in MATLAB/Simulink under various conditions to evaluate the electrical advantages of the proposed energy storage system.

References

- [1] Whittingham MS. History, evolution, and future status of energy storage. P IEEE 2012; 100: 1518-1534.
- [2] Vazquez S, Lukic SM, Galvan E, Franquelo LG, Carrasco JM. Energy storage systems for transport and grid applications. IEEE T Ind Electron 2010; 57: 3881-3895.
- [3] Boicea VA. Energy storage technologies: the past and the present. P IEEE 2014; 102: 1777-1794.
- [4] Díaz-González F, Del-Rosario-Calaf G, Girbau-Llistuella F, Gomis-Bellmunt O. Short-term energy storage for power quality improvement in weak MV grids with distributed renewable generation. In: IEEE PES Innovative Smart Grid Technologies Conference; 9–12 October 2016; Ljubljana, Slovenia. New York, NY, USA: IEEE. pp. 1-6.
- [5] Su HI, Gamal E. Modeling and analysis of the role of energy storage for renewable integration: power balancing. IEEE T Power Sys 2013; 28: 4109-4117.
- [6] Nourollah S, Pirayesh A, Fripp M. Multitier decentralized control scheme using energy storage unit and load management in inverter-based AC microgrids. Turk J Elec Eng & Comp Sci 2017; 25: 735-751.
- [7] Chemali E, Preindl M, Malysz P, Emadi A. Electrochemical and electrostatic energy storage and management systems for electric drive vehicles: state-of-the-art review and future trends. IEEE J Emerg Select Topics Power Electron 2016; 4: 1117-1134.

- [8] Khaligh A, Li Z. Battery, ultracapacitor, fuel cell, and hybrid energy storage systems for electric, hybrid electric, fuel cell, and plug-in hybrid electric vehicles: state of the art. *IEEE T Vehicle Tech* 2010; 59: 2806-2814.
- [9] Hannan M, Hoque M, Mohamed A, Ayob A. Review of energy storage systems for electric vehicle applications: issues and challenges. *Renew Sust Energy Rev* 2017; 69: 771-789.
- [10] Tang J, Fang J, Wen W. Superconducting magnetic bearings and active magnetic bearings in attitude control and energy storage flywheel for spacecraft. *IEEE T Appl Supercond* 2012; 22: 5702109.
- [11] Çelikel R, Özdemir M, Aydoğmuş Ö. Implementation of a flywheel energy storage system for space applications. *Turk J Elec Eng & Comp Sci* 2017; 25: 1197-1210.
- [12] Uno M, Tanaka K. Spacecraft electrical power system using lithium-ion capacitors. *IEEE T Aero Elec Sys* 2013; 49: 175-188.
- [13] Poullikkas A. A comparative overview of large-scale battery systems for electricity storage. *Renew Sust Energy Rev* 2013; 27: 778-788.
- [14] Wolfram P, Lutsey N. Electric Vehicles: Literature Review of Technology Costs and Carbon Emissions. Working Paper 2016-14. Washington, DC, USA: International Council on Clean Transportation, 2016.
- [15] Thounthong P, Chunkag V, Sethakul P, Davat B, Hinaje M. Comparative study of fuel-cell vehicle hybridization with battery or supercapacitor storage device. *IEEE T Vehicle Tech* 2009; 58: 3892-3904.
- [16] Mousavi S, Faraji F, Majazi A, Al-Haddad K. A comprehensive review of flywheel energy storage system technology. *Renew Sust Energy Rev* 2017; 67: 477-490.
- [17] González A, Goikolea E, Barrena J, Mysyk R. Review on supercapacitors: technologies and materials. *Renew Sust Energy Rev* 2016; 58: 1189-1206.
- [18] Naseri F, Farjah E, Ghanbari T. An efficient regenerative braking system based on battery/supercapacitor for electric, hybrid and plug-in hybrid electric vehicles with BLDC motor. *IEEE T Vehicle Tech* 2017; 66: 3724-3728.
- [19] Peña-Alzola R, Sebastián R, Quesada J, Colmenar A. Review of flywheel based energy storage systems. In: *International Conference on Power Engineering Energy and Electric Drives*; 11–13 May 2011; Malaga, Spain. New York, NY, USA: IEEE. pp. 1-6.
- [20] Meriam L, Kraige LG. *Engineering Mechanics: Dynamics*. 7th ed. New York, NY, USA: Wiley, 2012.
- [21] Park JD, Kalev C, Hofmann HF. Control of high-speed solid-rotor synchronous reluctance motor/generator for flywheel-based uninterruptible power supplies. *IEEE T Ind Electron* 2008; 55: 3038-3046.
- [22] Gengji W, Ping W. Rotor loss analysis of PMSM in flywheel energy storage system as uninterruptible power supply. *IEEE T Appl Supercond* 2016; 26: 1-5.
- [23] Kailasan A. Preliminary design and analysis of an energy storage flywheel. PhD, University of Virginia, Charlottesville, VA, USA, 2013.
- [24] Tang J, Fang J, Wen W. Superconducting magnetic bearings and active magnetic bearings in attitude control and energy storage flywheel for spacecraft. *IEEE T Appl Supercond* 2012; 22: 5702109.
- [25] Li X, Wei B. Supercapacitors based on nanostructured carbon. *Nano Energy* 2013; 2: 159-173.
- [26] Hadjipaschalis I, Poullikkas A, Efthimiou V. Overview of current and future energy storage technologies for electric power applications. *Renew Sust Energy Rev* 2009; 13: 1513-1522.
- [27] Xu Y. Kilowatt three-phase rotary transformer design for permanent magnet DC motor with on-rotor drive system. MSc, Mid Sweden University, Sundsvall, Sweden, 2016.
- [28] Hillers A, Christen D, Biela J. Design of a highly efficient bidirectional isolated LLC resonant converter. In: *15th International Power Electronics and Motion Control Conference*; 4–6 September 2012; Novi Sad, Serbia. New York, NY, USA: IEEE. pp. 1-8.
- [29] Genta G. *Kinetic Energy Storage: Theory and Practice of Advanced Flywheel Systems*. Amsterdam, the Netherlands: Elsevier Science, 2014.

- [30] Conteh M, Nsofor E. Composite flywheel material design for high-speed energy storage. *J Appl Res Tech* 2016; 14: 184-190.
- [31] Lei G, Zhu J, Guo Y. *Multidisciplinary Design Optimization Methods for Electrical Machines and Drive Systems*. 1st ed. Heidelberg, Germany: Springer-Verlag, 2016.
- [32] Maxwell Technologies. DuraBlue. K2 Ultracapacitors-2.85V/3400F. 3000619-EN.3 Datasheet. San Diego, CA, USA: Maxwell Technologies, 2015.
- [33] Lei G, Liu C, Zhu J, Guo Y. Robust multidisciplinary design optimization of PM machines with soft magnetic composite cores for batch production. *IEEE T Magn* 2016; 52: 1-4.